Elsevier Editorial System(tm) for Palaeogeography, Palaeoclimatology, Palaeoecology
Manuscript Draft

Manuscript Number:

Title: 3100 years of glacier and seismic activity in the Maladeta Massif (Central Pyrenees, Spain) recorded in proglacial Lake Barrancs sediments

Article Type: Special issue: Geolimnology

Keywords: Pyrenees; proglacial lakes; environmental magnetism; plant macrofossils; glacier fluctuations; paleoseismicity

Corresponding Author: Mr. Juan Cruz Larrasoana,

Corresponding Author's Institution: IES Jaume Almera

First Author: Juan C Larrasoana

Order of Authors: Juan C Larrasoana; Maria Ortuño; Josep M Parés; Hilary H Birks; Blas Valero-Garcés; Ramon Copons; Jaume Bordonau

Abstract: A combination of sedimentologic, mineral magnetic, and palaeobotanic techniques applied to a sediment core recovered from proglacial Lake Barrancs in the Maladeta Massif has provided the basis for documenting glacier and paleoseismic activity in the Central Pyrenees for the last ca. 3100 years. Deposition of Lake Barrancs responds to seasonal changes in sediment supply. Slow particle settling during the winter and the arrival of sediment-loaded homopycnal flows during the warm season, which are triggered by snowmelting and glacier outwash, hava resulted in deposition of rhythmites composed of clays, silts and sands. A comparison of the sedimentologic and magnetic record of Lake Barrancs with a regional record of climate variability suggests that relatively colder periods are characterized by coarser-grained sediments, preferential development of horizontal laminations, and larger concentrations of magnetite, which indicates simultaneous enhancement of glacier and homopycnal flow activity. Low magnetite concentrations and the predominance of poorly-laminated and finer-grained sediments before 200 B.C. suggest that glacier activity was significantly decreased, if not absent, before that time. After 200 B.C., important variations in the concentration of magnetite and the predominance coarser-grained laminated sediments suggest increased, but highly oscillating, glacier activity. In situ formation of two paleosoils at ca. 400 B.C. and A.D. 300 is indicative of dramatic lake level drops that interrupted lacustrine conditions. Geomorphological and structural evidence indicates that deformation of the valley bottom in response to glacier unloading after deglaciation resulted in active faulting, which played a prominent role in formation of Lake Barrancs. Our data support that the two inferred desiccation events could be seismically-induced through the reactivation of pre-existing faults by two earthquakes at ca. 400 years B.C. and A.D. 300.

Barcelona, June 18th 2008

Dear Lluis Cabrera, Elisabeth Gierlowski-Kordesch and Santiago Giralt,
Please find enclosed our manuscript entitled:

"**3100 years of glacier and seismic activity in the Maladeta Massif (Central Pyrenees, Spain) recorded in proglacial Lake Barrancs sediments**" by Juan C. Larrasoaña, Maria Ortuño, Josep M. Parés, Hilary H. Birks, Blas Valero-Garcés, Ramon Copons and Jaume Bordonau

for submission to **Palaeo 3.**

This paper deals with a sediment core drilled in proglacial Lake Barrancs (Maladeta Massif, central Pyrenees). We have used a combination of sedimentologic, environmental magnetic and paleobotanic techniques for identifying sedimentary processes governing sediment accumulation in the lake, which has provided the basis for disentangling glacier and paleoseismic activity in the Maladeta Massif for the last ca. 3100 years. We hope that it is of interest for the special volume of **Palaeo 3** committed to lake sediments.

We look forward to hearing from you.
Yours sincerely,
Juan Cruz Larrasoaña

Juan C. Larrasoaña
Department of Sedimentary Geology
IES Jaume Almera, CSIC
Solé i Sabarís s/n
08028 Barcelona
Spain
E-mail: jclarra@ija.csic.es
Tel: (+34) 93.409.54.10
Fax: (+34) 93.411.00.12

3100 years of glacier and seismic activity in the Maladeta Massif (Central Pyrenees, Spain) recorded in proglacial Lake Barrancs sediments

Juan C. Larrasoaña [a,*], María Ortuño [b], Josep M. Parés [c], Hilary H. Birks [d,e], Blas Valero-Garcés [f], Ramon Copons [b], Jaume Bordonau [b]

[a] *Institut de Ciències de la Terra "Jaume Almera", CSIC, Solé i Sabarís s/n, 08028 Barcelona, Spain*

[b] *RISKNAT Group, Departament de Geodinàmica i Geofisica, Universitat de Barcelona, Martí i Franqués s/n, 08028 Barcelona, Spain*

[c] *Department of Geological Sciences, University of Michigan, 2534 CC. Little Building, Ann Arbor, MI 48109-1063, USA. Now at: CENIEH, 09004 Burgos, Spain*

[d] *Department of Biology, University of Bergen, Allégaten 41, N-5007 Bergen, Norway*

[d] *Bierknes Centre for Climate Change, Allégaten 41, N-5007 Bergen, Norway*

[f] *Instituto Pirenaico de Ecología, CSIC, Aptdo. 13034, 50080 Zaragoza, Spain*

[*] Corresponding author. Tel.: +34 93 409 54 10; fax: +34 93 411 00 12. *E-mail address:* jclarra@ija.csic.es (J.C. Larrasoaña)

Abstract

A combination of sedimentologic, mineral magnetic, and palaeobotanic techniques applied to a sediment core recovered from proglacial Lake Barrancs in the Maladeta Massif has provided the basis for documenting glacier and paleoseismic activity in the Central Pyrenees for the last ca. 3100 years. Deposition of Lake Barrancs responds to seasonal changes in sediment supply. Slow particle settling during the winter and the arrival of sediment-loaded homopycnal flows during the warm season, which are triggered by snowmelting and glacier outwash, hava resulted in deposition of rhythmites composed of clays, silts and sands. A comparison of the sedimentologic and magnetic record of Lake Barrancs with a regional record of climate variability suggests that relatively colder periods are characterized by coarser-grained sediments, preferential development of horizontal laminations, and larger concentrations of magnetite, which indicates simultaneous enhancement of glacier and homopycnal flow activity. Low magnetite concentrations and the predominance of poorly-laminated and finer-grained sediments before 200 B.C. suggest that glacier activity was significantly decreased, if not absent, before that time. After 200 B.C., important variations in the concentration of magnetite and the predominance coarser-grained laminated sediments suggest increased, but highly oscillating, glacier activity. *In situ* formation of two paleosoils at ca. 400 B.C. and A.D. 300 is indicative of dramatic lake level drops that interrupted lacustrine conditions. Geomorphological and structural evidence indicates that deformation of the valley bottom in response to glacier unloading after deglaciation resulted in active faulting, which played a prominent role in formation of Lake Barrancs. Our data support that the two inferred desiccation events could be seismically-induced through the reactivation of pre-existing faults by two earthquakes at ca. 400 years B.C. and A.D. 300.

Keywords: Pyrenees; proglacial lakes; environmental magnetism; plant macrofossils; glacier fluctuations; paleoseismicity

1. Introduction

Lakes are important sedimentary archives of geological processes, paleoenvironmental variations, and past human activity because they have high accumulation rates that enable the study of these processes at resolutions down to centennial and even decadal timescales (see De Batist and Chapron, 2008). Among lake systems, high-altitude lakes are being the focus of an increasing number of studies because mountain belts are very sensitive to recent environmental variations (Battarbee et al., 2002; Pla and Catalan, 2005). This is especially the case for proglacial lakes, which have been shown to provide not only continuous, but also high-resolution records of glacier dynamics in locations where the geomorphological expression of environmental changes is very discontinuous both in time and space (Matthews and Karlén, 1992; Lemman and Niessen, 1994; Leonard and Reasoner, 1999; Dhal et al., 2003; Lie et al., 2004; Nesje et al., 2006; Chapron et al., 2007). The study of glacier dynamics from proglacial lake sediments is based on the assumption that glacier size controls sediment production and hence sediment transport into the lake (Lie et al., 2004; Nesje et al., 2006; Chapron et al., 2007). However, other processes such as fluvial reworking of glacial-sourced sediment load (e.g. the ´paraglacial` processes of Church and Ryder, 1972) might overprint the glacial signal (Lie et al., 2004).

Lake sediments have been also shown to provide long-term and well-dated records of seismic activity (Monecke et al., 2004; Becker et al., 2005; Carrillo et al., 2008; Wagner et al., 2008), which is important because other terrestrial paleoseismic indicators provide only discontinuous records of seismic activity that are difficult to date (Becker et al., 2005; De Batist and Chapron, 2008). In the last years, however, a growing number of studies are suggesting that the combined effect of seismic activity and environmental changes in lacustrine sedimentation might be a common phenomenon (Bertrand et al., 2008; Carrillo et al., 2008; Fanetti et al., 2008; Wagner et al., 2008). Thus, especial care has to be taken when studying lacustrine sedimentary records to disentangle signals of seismo-tectonic activity from those generated by climatic variability (De Batist and Chapron, 2008). This is especially relevant for high-altitude lakes because they are located in young and active mountain belts that are very sensitive to climatic variations and are affected by intense seismic activity.

Here we present the study of a 685 centimetres-thick sedimentary sequence recovered from proglacial Lake Barrancs, which is located at an altitude of 2360 m a.s.l. in the Maladeta Massif (Central Pyrenees, Spain). Lake Barrancs is one of the few Pyrenean lakes located just downstream (<1.5 km) of active cirque glaciers. Moreover, the Maladeta Massif is located in one of the most seismically active regions within the Pyrenean mountain belt (Souriau and Pauchet, 1998). The sedimentary sequence recovered from Lake Barrancs might therefore constitute a unique record of recent glacier and seismic activity in the Pyrenees. Mountain lakes, including proglacial lakes, are studied using a variety of techniques such as sedimentology (Monecke et al., 2004; Chapron et al., 2007; Paasche et al., 2007; Morellón et al., 2008), seismic stratigraphy (Monecke et al., 2004; Chapron et al., 2007), palynology (Lanci et al., 1999; Bennett and Willis, 2001; González-Sampériz et al., 2006), paleobotany (Birks, 1980), chemostratigraphy (Filippi et al., 1999; Moreno et al., 2007) and environmental magnetism (Snowball, 1991, 1993; Matthews and Karlén, 1992; Lanci et al., 1999; Zhu et al., 2003; Paasche et al., 2007), among others. Here we have used a combination of sedimentologic, environmental magnetic and paleobotanic techniques for identifying sedimentary processes governing sediment accumulation in Lake

Barrancs, which has provided the basis for disentangling environmental variations and paleoseismic activity in the Maladeta Massif for the last ca. 3100 years.

2. Geological setting

Lake Barrancs (2360 m a.s.l.) is located in the Axial Zone of the central Pyrenees, on the northern slope of the Maladeta Massif (Fig. 1). This massif hosts the highest Pyrenean peak (Aneto Peak, 3404 m a.s.l.) and the largest glaciers still preserved in the Pyrenean mountain belt (Fig. 2). The Maladeta Massif is composed of medium to coarse-grained granitoids emplaced within Paleozoic sediments in the late stages of the Variscan orogeny (Leblanc et al., 1994; Evans et al., 1998), and is affected by three sets of NNW-SSE, N-S, and WNW-ESE oriented subvertical fractures. Near Lake Barrancs, these fractures are represented by several NNW-SSE oriented fault scarps that have rectilinear traces and steep dips. They delineate an elongated ridge that separates two abrupt depressions, the easternmost one being occupied by Lake Barrancs and the westernmost one by periglacial talus (Figs. 1, 2). These faults show normal displacements of <40 m, have a maximum length of 1.4 km and in several, but not all cases, have glacial striae on their surfaces (Fig. 2c) (Moya and Vilaplana, 1992). These faults are located at about 7 km SW of the E-W trending North Maladeta fault. This 17.5 km long normal fault is the only seismogenic fault with geomorphological expression recognized in the central Pyrenees, and has been identified as the most likely source of historical earthquakes in the area, such as the M_W=5.3 Vielha (19.11.1923) and the M_W=6.2 Ribagorza (3.3.1373) earthquakes (Fig. 1a) (Ortuño et al., 2008).

During the Last Pyrenean Pleniglacial, recently dated to about 25-20 ka by means of ^{10}Be exposure ages (Pallàs et al., 2006), the Maladeta Massif was covered by a 36 km long valley glacier that flowed down the Esera valley. This glacier carved several overdeepened basins, such as the one where Lake Barrancs is located. Lake Barrancs likely formed during the final stages of the Pyrenean deglaciation, when the Esera glacier was fragmented into several cirque glaciers with small ice tongues. A moraine located just upstream of Lake Barrancs, at about 2400 m a.s.l. (Moya and Vilaplana, 1992; Copons and Bordonau, 1996), attests for the transient stabilization of these glaciers during the Pyrenean deglaciation (Figs. 1c, 2d). A maximum age of ca. 10 ka (e.g. Early Holocene) for this moraine is inferred on the basis of ^{10}Be exposure ages of moraines on the SE slope of the Maladeta Massif (Pallàs et al., 2006), which are considered older than that near Lake Barrancs based on geomorphological grounds. In addition, historical glacial phases have been documented in the Maladeta Massif. Thus, a prominent morainic ridge preserved near present cirque glaciers, including those located upstream of Lake Barrancs (Figs. 1c-d, 2b), attest for glacier advance during the Little Ice Age (LIA, 18 th-19th centuries) (Copons and Bordonau, 1994, 1996; Chueca et al., 2005).

Lake Barrancs (ca. 500 m long, 100 m wide and 13 m of maximum deep) constitutes a narrow, fault-bounded elongated lake located downstream of the Barrancs and Tempestats (0.11 and 0.14 km^2, respectively) cirque glaciers (Figs. 1, 2) (Copons and Bordonau, 1994, 1996; Chueca et al., 2005). The catchment of the lake (<4 km^2), including its outlet, is made up entirely of granitoids from the Maladeta Massif, and includes periglacial talus deposits and glacial tills that build up the Holocene and LIA moraines. The lake catchment has very strong topographic gradients (>1000 m in two km) and is largely snow covered from November to May, when frequent snow avalanches transport coarse material to the frozen surface of the lake. Snow melting in the catchment occurs typically between May and June. These melt waters erode and transport large amounts of Early Holocene and LIA till sediments, which has resulted in the formation of a proglacial cone downstream of the Barrancs glacier and of a delta in the southernmost part of Lake Barrancs, which occupies nearly half the depression where the lake is located (Figs. 1c-d, 2a). The eastern shore of Lake Barrancs is covered by screes, which have been generated by rockfalls from the overlying slopes that might often reach the lake bottom.

3. Materials and methods

Drilling in Lake Barrancs was carried out from the frozen surface of the lake in the winter of March 1998 (Fig. 2d). Twenty-one azimutally-unoriented cores, 6 cm in diameter and ranging from 69 to 100 cm in length, were recovered at five locations in the central part of the lake (Fig. 1, 2a). For this purpose, a stationary piston sampler equipped with a PVC core tube was used following Wright´s procedure (Wright, 1980). Results presented here come from one of the five locations, named core B5 and drilled at 12 m water depth, where seven consecutive cores comprise a nearly continuous sequence of 6.85 m in length.

In the laboratory, core B5 was split in two halves using an electric saw and a nylon thread for sedimentological description and sub-sampling. Total organic carbon content of some representative samples was determined using a LECO elemental analyzer at the IPE. Five samples were taken for AMS ^{14}C dating, which was performed at the Beta Analytic laboratory (Miami, USA). Three bulk samples and two samples in plant material were selected according to their stratigraphic position and lack of evidence of contamination. The AMS dates were calibrated with CALIB v.5.0.2 (Stuiver and Reimer, 1986; Stuiver et al., 2005).

Macrofossils were extracted from two samples (8 cm^3) of an organic-rich layer where plant remains were present. The samples were disaggregated in water and sieved through a 125 μm mesh. The remains of interest were systematically picked out at 12x magnification under a stereo-microscope and identified (Birks, 2001).

Sampling for environmental magnetic measurements was done by pushing 2x2x2 cm (8 cm^3) standard plastic boxes into the working half of core B5. Sampling was performed continuously through the sedimentary section, which gives a resolution of two cm. Magnetic properties were measured at the Paleomagnetic Laboratory of the Ludwig Maximilians Universität (Munich, Germany), and include: 1) the low field magnetic susceptibility (χ); 2) an anhysteretic remanent magnetization (ARM), applied in a dc bias field of 0.05 mT parallel to an axially-oriented peak alternating field (AF) of 100 mT; and 3) two isothermal remanent magnetizations applied at 0.2 T (IRM@0.2T) and 1.5 T (SIRM). χ was measured with a KLY-2 magnetic susceptibility bridge using a field of 0.1 mT at a frequency of 470 Hz. ARM was produced using a 2G Enterprises AF demagnetizer, and was measured with a 2G Enterprises three-axis cryogenic magnetometer (noise level of $<7 \times 10^{-6}$ A/m). The IRM@0.2T and SIRM were produced using a home-made pulse magnetizer and were measured also with the same 2G Enterprises cryogenic magnetometer. All magnetic properties were normalized by the dry weight of the samples. We have used different magnetic properties and interparametric ratios to determine downcore relative variations in the type, concentration and grain size of magnetic minerals (Thompson and Oldfield, 1986; Verosub and Roberts, 1995). χ has been used as a first order indicator for the concentration of magnetic (s.l.) minerals. SIRM/χ and the S-ratio (operationally defined as IRM@0.2T/SIRM; Bloemendal et al., 1992) have been used to detect changes in magnetic mineralogy (Verosub and Roberts, 1995; Peters and Dekkers, 2003). Then, the ARM and the "hard" IRM (HIRM, operationally defined as SIRM-IRM@0.2T; Thompson and Oldfield, 1986) have been used as a proxy for the concentration of low- and high-coercivity minerals, respectively (Verosub and Roberts, 1995). Finally, ARM/SIRM has been used to detect downcore changes in magnetic grain size, provided that they correspond to a single magnetic mineral (Verosub and Roberts, 1995; Larrasoaña et al., 2003). All results from core B5 are referred to centimetres below the lake floor (cblf).

4. Results

4.1. Lithostratigraphy, TOC, macrofossil, and AMS ^{14}C data of core B5

Core B5 includes a nearly continuous sequence of proglacial sediments that are characterized by three main sedimentary facies (Fig. 3). Facies F1 is composed of light brown to grey clays, silts and sandy silts that contain occasional organic debris forming discrete mm-thick intervals. Facies F1 sediments have a poorly developed horizontal lamination that is mainly marked by faint colour and textural variations. Facies F2 is composed of light brown to grey clay and silts that contain isolated organic debris and include abundant layers of sandy silts and fine sands. The sandy silts and fine sands occasionally contain distinctive whitish layers, which can be up to 1 cm thick and often show a fining-upward textural gradation. Facies F2 sediments have a well-developed millimetric to centimetric horizontal lamination that is marked by textural and colour variations. Intervals composed by facies F2 dominate between 430 and 150 cblf, and became scarce specially in the lowermost 3 m of the record. Apart from intervals containing organic fragments, selected samples representative for facies F1 and F2 have low TOC contents (<0.4 % in weight, Table 1). It is worth mentioning that, although no dropstone has been observed throughout the studied sequence of core B5, the presence of dropstones in Lake Barrancs sediments is evidenced by the difficulties faced when drilling other cores, which had to be abandoned when PVC core tubes encountered large blocks that damaged their tips and prevented further drilling.

Between 344 and 363 cblf, a distinctive dark layer (facies F3) appears intercalated within a thick (70 cm) facies F2 interval (Fig. 3). This 19-cm thick layer is composed of silts and sands, which include large quartz, feldspar and biotite grains of up to 3 mm at the base of the layer. The distinctive dark colour is given by disseminated organic matter and mm-scale vegetal remains, which give a mean TOC content of nearly 3 % in weight (Table 1). At the top of the layer, roots are preserved in a vertical position and penetrate down to 10 cm within the layer. Identification of plant macrofossils in two samples from this layer give an association composed of *Calluna vulgaris*, *Rhododendruon ferrugineum*, *Selaginella selaginoides, Juniperus communis*, *Salix* sp., *Betula (peduncula/pubescens)*, *Ranunculus* sp., and *Carex* sp., and an associated fauna of oribatids, trichopterids, chironomids and fragments of other insects (Table 2). This association is typical for Pyrenean heathlands located around mountain streams up to 2200 m a.s.l. (Villar et al., 1997). Between 424-427 cblf, another distinctive dark, organic-rich layer appears at the base of a thin (20 cm) facies F2 interval (Fig. 3). This layer is also composed of silts and sands that contain organic debris (including root fragments) and large quartz, feldspar, and biotite grains (<2 mm) in its lower part.

The five AMS dates give ages that range between 2560 ± 40 ^{14}C yr BP in the lowermost sample (Beta-122149, 567 cblf) and 1240 ± 40 ^{14}C yr BP in the uppermost sample (Beta-122150, 170 cblf), with one inverted age in sample Beta-122151 (286.5 cblf) (Table 3). This sample has been excluded for developing the age-depth model of core B5, which is based on linear interpolation between calibrated radiocarbon dates (Fig. 4). Linear interpolation down from the lowermost two samples gives an age of ca. 1100 B.C. for the base of the sequence recovered in core B5. This gives a mean accumulation rate of 2.2 mm/year, which is similar to that reported previously from Lake Barrancs (e.g. 2.6 mm/year; Copons et al., 1997) and is therefore several times larger than those of other high-altitude Pyrenean lakes such as Lake Tramacastilla (ca. 0.4 mm/year; García-Ruiz et al., 2003) or the neighbouring Lake Redon (ca. 0.055 mm/year; Pla and Catalán, 2005) regardless of catchment surface or rock type.

4.2. Environmental magnetism

Magnetic susceptibility values oscillate around 8 x 10^{-8} m^3/kg throughout the record but in the two organic rich layers at around 350 and 430 cblf and at a facies F1 interval located around 650 cblf, where magnetic susceptibility values drop sharply to well below 7 x 10^{-8} m^3/kg (Fig. 3). These values are very similar to those of samples from the Maladeta granitoid, which typically range between 10 and 30 x 10^{-5} SI (Leblanc et al., 1994). This is consistent with the fact that the granitoid rocks that constitute the entire catchment of Lake Barrancs, which are dominantly paramagnetic (Leblanc et al., 1994), are the main source for sediments accumulated in Lake Barrancs. Low magnetic susceptibility values such as those in the two organic-rich layers might indicate a different concentration of detrital minerals or, alternatively, a postdepositional change in the primary magnetic signal.

Facies F1 and F2 are characterized by S-ratios ranging between 0.7 and 0.9, which contrast with the distinctively low (down to 0.6) S-ratios in the two organic-rich layers (facies F3) (Fig. 4). SIRM/χ values oscillate between 0.5 and 3.5 kA/m except in the uppermost organic-rich layer, which shows distinctively high SIRM/χ values of up to 9 kA/m. Such high S-ratios combined with distinctively low SIRM/χ values indicate that the main magnetic mineral characterizing facies F1 and F2 is magnetite (Snowball, 1993; Peters and Dekkers, 2003; Verosub and Roberts, 1995). This magnetite is mainly derived from glacial abrasion of the granitoid catchment rock and its subsequent transport to the lake mainly by snow-melt waters and glacier outwash. Downcore variations in ARM intensity reveal a rather low ($<2 \times 10^{-6}$ Am^2/kg) and constant concentration of magnetite in the lower 3 m of the core, which contrast with oscillating values between 2×10^{-6} and 10×10^{-6} Am^2/kg from 400 cblf upwards. ARM/SIRM values show a similar trend, being lower (around 0.02) and relatively homogeneous downwards from 400 cblf and larger, but highly oscillating (0.02-0.04), in the uppermost 4 m of the record. This change in magnetic behaviour at 400 cblf is also evidenced by S-ratios, which are significantly lower (0.77 ± 0.04) and higher (0.85 ± 0.03) below and above that depth, respectively. It seems that magnetic parameters are related to sedimentary facies. Facies F2 intervals, which are dominant in the upper 4.3 m of the record, are often characterized by slightly higher S-ratios and larger concentrations (higher ARM values) of relatively finer-grained (higher ARM/SIRM ratios) magnetite grains compared to facies F1. Facies F1 dominates the lower 2.7 m of the record, which are characterized by lower S-ratios and low concentrations (low ARM) of relatively coarser-grained (low ARM/SIRM ratios) magnetite.

The distinctively low S-ratios that characterize the two organic rich layers indicate that the main magnetic mineral present in facies F3 is not magnetite, but rather a higher-coercivity mineral phase (Verosub and Roberts, 1995). Diagenetic reactions in sediments are mainly driven by the metabolic activity of microbes, which consume oxygen (under oxic conditions), nitrate, manganese and iron oxides (under suboxic conditions), and sulphate (under anoxic conditions) to degrade buried organic matter (Froelich et al., 1979). Microbially-mediated reduction of sulphate during earliest diagenesis releases sulphide, which reacts with iron-bearing minerals (including magnetic grains) and dissolved iron to form iron sulphides. Significant accumulations of organic matter in lake sediments easily drives diagenetic reactions to the point where detrital magnetic grains are dissolved and the magnetic iron sulphide greigite is formed (Snowball, 1991). This process is favoured when sulphide is produced in low amounts (e.g. Larrasoaña et al., 2007), which typically happens in small lakes due to the low availability of dissolved sulphate. Given the high organic content of the two organic-rich layers, and keeping in mind that hematite and goethite are unstable under reducing conditions (Canfield et al., 1992), we interpret that the most likely magnetic mineral in F3 sediments is greigite because it better explains the combined lower S-ratios and distinctively higher SIRM/χ values (Snowball, 1991, 1993; Roberts, 1995) of the two organic-rich layers. Authigenic growth of greigite and reductive dissolution of magnetite accounts for the low χ values of the organic-rich layers, because magnetite has a larger specific magnetic susceptibility compared to greigite (Roberts, 1995). HIRM values give an indication of the concentration of relatively high coercivity minerals, and therefore indicate that large amounts of greigite formed in the uppermost organic-rich layer, but not in the lowermost one.

5. Discussion

5.1. Sedimentary processes in Lake Barrancs

Facies F1 and F2 described for core B5 are typical for proglacial lakes in which rhythmic sedimentation is controlled by the seasonal alternation of intense snow and glacier melting during the spring and summer with freezing conditions over the winter and early spring (Ashley, 1995; Chapron et al., 2007). During the late spring and the early summer, specially between May and June, sudden periods of snow melting cause cold and sediment-loaded runoff waters to flow into the lake. They form an underflow current that is gradually mixed with the lake water. Over the course of the summer, glacier outwash takes over as the main source of underflow currents. As a result of these currents, also called homopycnal flows (Bates, 1954), the sedimentary load moves by advection throughout the water column until it eventually settles down draping the lake bottom (Ashley, 1995, Chapron et al., 2007). Homopycnal flows are an effective mechanism for separating relatively coarser- and finer-grained sediments due to their differential settling times (Ashley, 1995), which accounts for the alternation of clays, silts and sands that characterizes facies F1 and F2. During winter and early spring, when the surface of the lake is frozen, sedimentation is restricted to the settling of the finer particles still in suspension, which accounts for the presence of thin clay layers within facies F1 and F2 sediments. The higher abundance of sandy silts and fine sands in facies F2 is interpreted to respond to an increased intensity and/or frequency of homopycnal flows through time (Chapron et al., 2007), and might also explain the better-developed laminations in sediments displaying facies F2.

Frequent episodes of snow and glacier melting throughout the spring and summer, coupled with the availability of easily erodable morainic material in the catchment, might explain the extremely high accumulation rates (2.2 mm/year) that characterize the studied sediments of Lake Barrancs. In this regard, it is worth mentioning that a substantial part of the sedimentary load produced by the Barrancs and Tempestats glaciers is trapped in the proglacial cone formed downstream of the Barrancs glacier and the delta that occupies the proximal part of Lake Barrancs (Fig. 1, 2a). Despite this, intense glacial grinding together with meltwater runoff and erosion of glacial deposits provides a very effective mechanism for transferring sedimentary load from the glaciated areas of the catchment into Lake Barrancs. The dominance in the uppermost 4.2 m of the record of facies F2, which are enriched in graded, coarser-grained and laminated sediments with respect to facies F1, suggests an increase in meltwater flow into Lake Barrancs likely as a result of higher glacier and snowmelt activity in the catchement.

Facies F3 described for the two organic-rich layers of core B5 is indicative of paleosoil formation under subaerial conditions, although the presence of aquatic invertebrates and *Selaginella* might indicate sporadic (e.g. seasonal) flooding. At least for the organic-rich layer at around 350 cblf, the plant macrofossil assemblage indicates that subaerial conditions lasted long enough to enable development of a dwarf shrub and tree community and accumulation of some peat. This period of paleosoil formation, which can be of the order of one hundred years or more, is consistent with decreased accumulation rates observed around the two organic-rich layers between 340 and 430 cblf (Fig. 4). Since core B5 was drilled near the deepest part of the lake, formation of these paleosoils implies dramatic lake-level drops. It might be argued that these two organic rich-layers correspond to reworked peat and paleosoil fragments that were transported by snow avalanches or slid from the deltaic plain located upstream. We discard these possibilities and propose that the two organic rich-layers actually constitute paleosoils formed in situ because: 1) the presence of roots in a vertical position and the absence for internal deformation is not consistent with a slump (e.g. folded) geometry; 2) deposition of slid sediments would cause an spurious increase in accumulation rates, which is just opposite to the decreased accumulation rates observed around the two organic-rich layers; and 3) the basal part of the two organic-rich layers contain the coarsest sand grains reported in the section (Fig. 3), which is compatible with the inferred sudden base level falls and the concomitant arrival of coarser detrital material.

5.2. Paleoenvironmental implications

We have used both ARM intensities and ARM/SIRM ratios as proxies for the amount and magnetic grain size of detrital magnetite in facies F1 and F2 sediments. For unravelling the paleoclimatic significance of these two records, downcore variations of such proxies have been compared with the sequence of Late Holocene global climatic variations recognized at different locations throughout the Iberian Peninsula (Gutiérrez-Elorza and Peña-Monné, 1998; Riera et al., 2002; Desprat et al., 2003; Gil-García et al., 2007) (Fig. 5). No obvious correlation is found between magnetic parameters and climatic events. Relatively warm and wet events such as the Subboreal Climate Optimum (<975 B.C.), the Roman Warm Period (250 B.C.-A.D. 450) and the Medieval Warm Period (A.D. 950-A.D. 1400) have both high and low ARM and ARM/SIRM values. Similarly, colder periods such as the Subatlantic Cold Period (975 B.C.-250 B.C.), the Dark Ages (A.D. 450-A.D. 950) and the Little Ice Age (A.D. 1400-A.D. 1850) also correspond to peaks and lows in ARM and ARM/SIRM. This lack of correlation might be related to the difficulties in linking globally-established climatic events with environmental changes at a specific mountain location with its own physiographic and environmental responses to climate change.

We have also compared the Lake Barrancs record with a regional record of climate variability based on chrysophyte cysts from the neighbouring Lake Redon (Fig. 5) (Pla and Catalán, 2005), which is located just ca. 8 km east of Lake Barrancs at a similar altitude (2240 m a.s.l.). Since distribution of chrysophyte cysts is related mainly to altitude, downcore variations in chrysophyte cists have been used to estimate a local altitude anomaly that reflects changes in winter mean temperatures through time (negative and positive altitude anomalies indicate warmer and colder temperatures, respectively) (Pla and Catalan, 2005). The Lake Redon record shows rather small winter temperature anomalies (WTA) between 1200 B.C. and A.D. 1000, when mean winter temperatures usually oscillated between 0.2ºC warmer and –0.4ºC colder than present. This period is punctuated by one cold interval (WTA = –0.6ºC) at around A.D. 0 and three warm intervals around A.D. 400, A.D. 650 and A.D. 950 (WTA = 0.3ºC). Mean winter temperatures after A.D. 950 experienced a rapid decrease of ca. 1.4ºC in 100 years, being 1.1ºC colder than today by A.D. 1050. From A.D. 1050 to the present, mean winter temperatures show a progressive warming trend that is characterized by large-amplitude oscillations of up to 1ºC/100 years.

The ARM and ARM/SIRM records from Lake Barrancs do not show a clear long-term correlation with mean winter temperatures. Thus, some relatively warmer intervals (e.g. A.D. 600-A.D. 100) coincide with peaks in ARM and ARM/SIRM values whereas others (e.g. 1000 B.C.-400 B.C) correspond with ARM and ARM/SIRM lows (Fig. 5). In the short-term, however, magnetic parameters show an apparent negative correlation with winter mean temperatures, in such a way that short-lived cold intervals (e.g. at A.D. 0, A.D. 800, A.D. 1350, A.D. 1500, A.D. 1950) correlate with relative maxima in ARM and ARM/SIRM. Similarly, intervening warm periods (e.g. at 300-900 B.C., A.D. 200, A.D. 950, A.D. 1400) correspond to relative lows in ARM and ARM/SIRM. The correspondence between increased ARM values and relatively colder mean winter temperatures suggests an increase in detrital supply as a result of lowered equilibrium line altitude (ELA) and enhanced glacier activity during cold periods (Paterson, 1994), which is consistent with results from other proglacial lake records (Dhal et al., 2003; Lie et al., 2004; Nesje et al., 2006; Chapron et al., 2007). It is very likely that part of the increase in magnetite concentration is due to the higher frequency and intensity of meltwater events, because they likely relate to the amount of winter precipitation (Paasche et al., 2007) and, therefore probably, to winter mean temperatures. This explains the apparent correlation between high ARM values and facies indicative of enhanced homoycnal flow activity (Fig. 3). It appears, therefore, that glacial activity and enhanced fluvial transport of sediment load operated in phase and responded rapidly to climate fluctuations.

The correspondence of increased ARM/SIRM values, and hence of finer magnetite grains, with colder winter mean temperatures is difficult to explain because both glacier and homopycnal flow activity are typically manifested by coarser grain sizes (Lie et al., 2004; Nesje et al., 2006; Paasche et al., 2007; Chapron et al., 2007). There are two main alternative explanations for this discrepancy: 1) coarser magnetite grains during warmer periods respond to reductive dissolution of detrital magnetite, a process that affects preferentially to the finer fractions (e.g. Larrasoaña et al., 2003) and that has been reported from other glaciolacustrine sequences (Snowball, 1993); and 2) finer magnetic grains during colder periods result from additional production of single-domain magnetite by magnetotactic bacteria, a process that has been also reported in other glaciolacustrine records (Snowball, 1994; Snowball et al., 1999). Decreased lake water mixing as a result of reduced homopycnal flow activity during warm periods might have favoured anoxic conditions in the lake floor, trigging reductive dissolution of magnetite. Similarly, production of bacterial magnetite might have been favoured during cold periods in response to enhanced homopycnal flow activity and increased nutrient availability. In the absence of conclusive evidence, we interpret that both reductive dissolution and bacterial production of magnetite might have been operative during accumulation of Lake Barrancs sediments, because both are common in mountain lakes and account for the magnetic properties of both facies F1 and F2. In this regard, we notice that reductive dissolution of magnetite during warm periods and bacterial production of magnetite during cold periods might overprint the ARM signal. This might explain why ARM values do not significantly rise coinciding with a very short cold period evidencing the LIA (at around A.D. 1800, Fig. 5), despite the fact that the most prominent glacial deposits in the catchment of Lake Barrancs accumulated during this period (Fig. 1) (Copons and Bordonau, 1994, 1996; Chueca et al., 2005). In any case, the broad correspondence of high ARM intensities with facies indicative of enhanced meltwater runoff suggests that at least part of the ARM record represents a genuine detrital signal.

The predominance of facies F2 in the uppermost 4.2 m of the record, combined with overall increased (but highly oscillating) ARM values from about the same depth upwards (400 cblf), suggests that meltwater runoff as a result of snowmelt and glacier outwash has been a common phenomenon in the catchment of Lake Barrancs for at least since ca. 200 B.C. (Fig. 5). Given that the warmest periods of the last 2200 years are characterized by WTA of <0.3ºC compared to present (Pla and Catalán, 2005) (Fig. 5), it is likely that at least small cirque glaciers such as those preserved nowadays persisted in the catchment of Lake Barrancs during these only slightly warmer periods. Before 200 B.C., the predominance of facies F1 combined with low and constant ARM values suggests a significant decrease in meltwater runoff. Moreover, S-ratios before 200 B.C. show a marked change to slightly lower values, which might indicate prolonged periods of magnetite dissolution in response to sustained warm conditions. These circumstances suggest that glacier activity was significantly decreased, if not absent, between 200 B.C. and at least 1100 B.C., which is the lower boundary of our record. Earlier than 1100 B.C., significantly cold winters (WTA > -1ºC) are not found in the Lake Redon record till back to 6000 B.C. (Pla and Catalán, 2005). This suggests that glacial activity between 1100 B.C. and 6000 B.C. was also significantly reduced, and supports the inferred Early Holocene age for the phase of glacier advance marked by the moraine found just upstream of Lake Barrancs.

5.2. Paleoseismic implications

Formation of the two paleosoils at ca. 400 B.C. and A.D. 300 evidences dramatic lake level drops that, keeping in mind that core B5 was drilled near the deepest part of the lake, imply a nearly complete desiccation of Lake Barrancs. Since the outlet of the lake is entirely composed of catchment rocks from the Maladeta granitoid, catastrophic desiccation of the lake in response to landsliding of the outlet is not a feasible mechanism. A comparison with the paleoclimate proxy produced from Lake Redon reveals that the two paleosoils of Lake Barrancs formed during periods with positive winter temperature anomalies (Fig. 5). Especially significant is the temperature anomaly associated with the uppermost paleosoil (WTA = +0.3ºC), which indicates that it formed during the warmest periods of the last 3100 years. It is worth noticing that the equivalent altitude anomaly for this WTA is of ca. 60 m lower than present (ca. 2300 m a.s.l., see Pla and Catalán, 2005), which is broadly consistent with the upper altitudinal boundary for the plant macrofossil association found in the paleosoil (ca. 2200 m a.s.l.). Although this warm period might have favoured an increase in evaporation, it is unlikely to have reached the point of causing nearly complete desiccation of the lake.

In order to find an alternative explanation for the formation of the two paleosoils, we need to consider the tectonic and geomorphologic setting of Lake Barrancs. The faults that delineate the lake basin offset glacial polished surfaces attributed to the Last Pyrenean Pleniglacial, and have glacial striae on their surface (Moya and Vilaplana, 1992). Other faults, such as those located just near the SW shore of Lake Barrancs and those located downstream of the Aneto glacier (Fig. 1c), do not have glacial striae on their surface. Moreover, one of such faults without glacial striae is fossilized by a LIA moraine of the Aneto Glacier despite of being located near the present-day glacier front. This suggests that faulting around Lake Barrancs has been active at different times since the Last Pyrenean Pleniglacial (20-25 ka. Pallàs et al., 2006) up to nearly the LIA (Moya and Vilaplana, 1992). Concerning their mechanism of formation, their length of <1.4 km is well below the lower boundary for rupture length of seismogenic faults (~3.8 km for normal faults, Wells and Coppersmith, 1994). The location of the faults near the bottom of the valley makes a gravitational origin also unlikely (Moya and Vilaplana, 1992). A more plausible explanation for these faults is the uplift of the valley bottom in response to vertical unloading following overdeepening and melting of the Esera glacier. This mechanism has been proposed by other authors to interpret similar features in alpine environments (Mollard, 1977, Ego et al., 1996; Persaud and Pfiffner, 2004), and has been shown to be capable of generating scarps more than 10 m high in the slopes of the Rhine valley (Swiss Alps) (Ustaszewski et al., 2008). According to numerical models, this effect is observed along subvertical pre-existing faults for ice thicknesses between 400 and 1225 m and deglaciation periods ranging from 1 to 10 kyr (Ustaszewski et al., 2008). We suggest that this mechanism explains the formation of faults scarps along pre-existing fractures near Lake Barrancs, where ice thicknesses likely exceeded 300 m and deglaciation occurred in a short time period of <10 kyr (Pallàs et al., 2006).

Since geomorphological and structural evidence indicates that active deformation of the valley bottom in response to glacier unloading after the Last Pyrenean Pleniglacial has played a prominent role in the formation of the Barrancs basin, we propose that the most reliable explanation for the two sudden desiccation events is that Lake Barrancs was emptied through a pre-existing fracture network reactivated by earthquakes. Such a hypothesis is reinforced by the record of historical and prehistorical seismic activity along the neighbouring North Maladeta Fault (Ortuño et al., 2008). The rapid transition from the paleosoils back to facies F2 sediments indicates that lacustrine conditions were rapidly re-established, which is consistent with a scenario of rapid sealing of the fractures acting as a subaquatic outlet by sediments dragged by the outflowing water. If our interpretation is correct, then the Lake Barrancs record shows evidence for the occurrence of two seismic events along the North Maladeta Fault in the region at ca. 400 B.C. and A.D. 300, which is compatible with the geomorphological and historical evidence for faulting activity as recent as nearly the LIA (Moya and Vilaplana, 1992; Ortuño et al., 2008) (e.g. A.D. 1820; Copons and Bordonau, 1994, 1996; Chueca et al., 2005). Given the particularity of the sedimentological expression of these seismic events (e.g. formation of paleosoils), we consider that no interpretation can be made on the intensity of the putative earthquakes. It is thus possible, for instance, that a small seismic event sufficed to open a preexisting fracture and causing drainage of the lake, and that a larger earthquake did not result in significant fracture opening. This seems to be the case for the historical Vielha (M_W = 5.3, A.D.1923) and the Ribagorza (M_W = 6.2, A.D. 1373) earthquakes, which are not manifested in the Lake Barrancs record by any period of paleosoil formation (Fig. 5).

5.3. Recent glacier and seismic activity in the Maladeta Massif

Based on the results from core B5 and on previous studies (Moya and Vilaplana, 1992; Copons and Bordonau, 1994, 1996; Chueca et a., 2005; Pla and Catalan, 2005), the recent history of glacier and seismic activity in the Maladeta Massif can be summarized as follows (Fig. 6). During the Last Pyrenean Pleniglacial, the Barrancs basin was carved by the Barrancs glacier, which reached a thickness of around 400 m (Fig. 6a). At some time between the Last Pyrenean Pleniglacial (25-20 ka) and the Early Holocene (e.g. 8-10 ka), melting of the Barrancs glacier led to uplift of the bottom valley and formation of a horst and two adjacent grabens along pre-existing fractures of the Maladeta Massif. The easternmost of these grabens was occupied by Lake Barrancs (Fig. 6b). The faults that delineate the Lake Barrancs basin have glacial striae on their surface, which attest for an earlier period of glacial advance that likely occurred during the Younger Dryas cold period and that postdates formation of the faults. Rapid deglaciation after 8-10 ka led to reduced, if not absent, glacier activity in the catchment of Lake Barrancs in response to sustained warm temperatures up to 200 B.C. (Fig. 6c). Reactivation of fractures in response to seismic shaking led to transient desiccation of Lake Barrancs and formation of the lowermost paleosoil at 400 B.C. Glacier activity significantly increased at 200 B.C. onwards, when glacier size likely suffered important oscillations. In any case, it is likely that at least small cirque glaciers persisted in the catchment of Lake Barrancs during the warmest intervening periods (Fig. 6d).

During one of these warm periods at A.D. 300, a new earthquake led to reactivation of some fractures (P_1 and P_2), including those that caused desiccation of Lake Barrancs (Fig. 6d). Glacier advance during the LIA led to the fossilization of some of these fractures (e.g. P_1). Seismic activity after subsequent glacial retreat must have occurred till very recently, perhaps related to the Ribagorza earthquake (Fig. 5), as suggested by the later formation of other fractures (such as that located near the present day front of the Aneto glacier; Fig. 1c) that do not have glacial striae on their surface.

6. Conclusions

The studied sequence recovered from proglacial Lake Barrancs is composed of three sedimentary facies. Facies F1 and F2 are made up by clays, silts, and sands that have low (< 0.4 %) TOC contents, whereas facies F3 is composed of organic-rich (TOC ~ 3 %) silts and sands that form two distinctively dark layers at 344-363 and 424-427 centimetres below the lake floor (cblf). Facies F1 and F2 respond to seasonal changes in sediment supply, which is characterized by slow particle settling during the winter and by the arrival of sediment-loaded homopycnal flows, triggered by snowmelting and glacier outwash, during the warm season. Plant macrofossil assemblages and the presence of roots in a vertical position indicate that facies F3 represents *in situ* formation of two paleosoils at ca. 400 B.C. and A.D. 300. Combined low IRM/χ values and high S-ratios indicate that magnetite is the main magnetic mineral in facies F1 and F2. Higher magnetite contents, indicated by high ARM values, are preferentially associated to facies F2, which is enriched in coarser-grained sediments and displays better-developed horizontal laminations compared to facies F1. A comparison of the sedimentologic and magnetic record of Lake Barrancs with a regional record of climate variability suggests that relatively colder periods are characterized by coarser-grained sediments, preferential development of horizontal laminations, and larger concentrations of magnetite, which points to simultaneous enhancement of glacier and homopycnal flow activity. Low magnetite concentrations and the predominance of facies F1 sediments before 200 B.C. suggest that glacier activity was significantly decreased, if not absent, before that time. After 200 years B.C., important variations in the concentration of magnetite and the predominance of facies F2 sediments suggest increased, but highly oscillating, glacier activity. Combined high IRM/χ and low S-ratios of facies F3 indicates that greigite likely formed authigenically during degradation of organic matter in the two paleosoils, which are indicative of sudden lake level drops. Since geomorphological and structural evidence indicates that formation of the Barrancs basin is related to active deformation of the valley bottom in response to glacier unloading during the Pyrenean deglaciation (20-10 kyr), we propose that the most reliable explanation for the two sudden desiccation events is that Lake Barrancs was emptied through a pre-existing fracture network reactivated by earthquakes at ca. 400 years B.C. and A.D. 300, which is consistent with the widespread evidence of historical seismic activity in the area. Our results strengthen the view that proglacial lakes constitute excellent archives of past glacier fluctuations, and suggests that they might also provide a reliable record of seismic activity in young and active mountain belts. Our results also indicate that the combined effect of seismic activity and environmental changes on sedimentation in mountain lakes might be a common phenomenon.

Acknowledgements. We are very grateful to our colleagues of the Paleomagnetic Laboratory of the Ludwig-Maximilians Universität (Munich, Germany), where the rockmagnetic analyses were carried out, for their hospitality, technical assistance and discussion at the early stages of this study. This research was supported by a MEC Ramón y Cajal contract (JCL). We are also very grateful to Jordi Catalán, who kindly provided results from Lake Redon.

References

Ashley, G.M., 1995. Glaciolacustrine environments. In: Menzies, J. (Ed.), Modern Glacial Environments: Processes, Dynamics and Sediments. Butterworth-Heinemann Ltd., pp. 417-444.

Barttabee, R.W., Grytness, J.A., Thompson, R., Appleby, P.G., Catalan, J., Korhola, A., Birks, J.B., Lami, A., 2002. Climate variability and ecosystem dynamics at remote alpine and arctic lakes: the last 200 years. J. Paleolimnol. 28, 161-179.

Bates, C.C., 1954. Rational theory of delta formation. AAPG Bulletin 37, 2219-2162.

Becker, A., Ferry, M., Monecke, K., Schnellmann, M., Giardini, D., 2005. Multiarchive paleoseismic record of late Pleistocene and Holocene strong earthquakes in Switzerland. Tectonophysics 400, 153-177.

Bennett, K.D., Willis, K.J., 2001. Pollen. In: Smol, J.P., Birks, H.J.B., Last, W.M. (Eds.), Tracking Environmental Change using Lake Sediments, Volume 3: Terrestrial, Algal, and Siliceous Indicators. Kluwer Academic Publishers, Dordrecht, The Netherlands, pp 5-32.

Bertrand, S., Charlet, F., Chapron, E., Fagel, N., De Batist, M., 2008. Reconstruction of the Holocene seismotectonic activity of the Southern Andes from seismites recorded in Lago Icalma, Chile, 39ºS. Palaeogeogr. Palaeoclimatol. Palaeoecol. 259, 301-322.

Birks, H.H. 1980. Plant macrofossils in Quaternary lake sediments. Archiv für Hydrobiologie 15, 60 pp.

Birks, H.H., 2001. Plant macrofossils. In: Smol, J.P., Birks, H.J.B., Last, W.M. (Eds.), Tracking Environmental Change using Lake Sediments, Volume 3: Terrestrial, Algal, and Siliceous Indicators. Kluwer Academic Publishers, Dordrecht, The Netherlands, pp.49-74.

Bloemendal, J., King, J.W., Hall, F.R., Doh, S.J., 1992. Rock magnetism of Late Neogene and Pleistocene deep-sea sediments: relationship to sediment source, diagenetic processes and sediment lithology. J. Geophys. Res. 97, 4361-4375.

Canfield, D.E., Raiswell, R., Bottrell, S.H., 1992. The reactivity of sedimentary iron minerals toward sulfide. Am. J. Sci. 292, 659-683.

Carrillo, E., Beck, C., Audemard, F.A., Moreno, E., Ollarves, R., 2008. Disentangling Late Quaternary climatic and seismo-tectonic controls on Lake Mucubají sedimentation (Mérida, Andes, Venezuela). Palaeogeogr. Palaeoclimatol. Palaeoecol. 259, 284-300.

Chapron, E., Faïn, X., Magand, O., Charlet, L., Debret, M., Mélieres, M.A., 2007. Reconstructing recent environmental changes from proglacial lake sediments in the western Alps (Lake Blanc Huez, 2543 m a.s.l., Grandes Rousses Massif, France). Palaeogeogr. Palaeoclimatol. Palaeoecol. 252, 586-600.

Chueca Cía, J., Julián Andrés, A., Saz Sánchez, M.A., creus Novau, J., López Moreno, J.L., 2005. Responses to climatic changes since the Little ice Age on Maladeta Glacier (Central Pyrenees). Geomorphology 68, 167-182.

Church, M., Ryder, J.M., 1972. Paraglacial sedimentation: a consideration of fluvial processes conditioned by glaciation. Geol. Soc. Am. Bull. 83, 3059-3072.

Copons, R., Bordonau, J., 1994. La Pequeña Edad del Hielo en el macizo de la Maladeta (Alta cuenca del Ésera, Pirineos centrals). In: Martí-Bono, C., García-Ruiz, J.M. (Eds.), El Glaciarismo Surpirenaico: Nuevas Aportaciones. Geoforma Ediciones, Logroño, Spain, pp. 111-124.

Copons, R., Bordonau, J., 1996. El ultimo ciclo glaciar (Pleistoceno superior-Holoceno) en el macizo de la Maladeta (Pirineos Centrales). Rev. Soc. Geol. Esp. 10, 55-66.

Copons, R., Parés, J.M., Dinarès-Turell, J., Bordonau, J., 1997. Sampling induced AMS in soft sediments: a case study in Holocene glaciolacustrine rhythmites from lake Barrancs (Central Pyrenees, Spain). Phys. Chem. Earth 22, 137-141.

De Batist, M., Chapron, E., 2008. Lake systems: sedimentary archives of climate change and tectonics. Palaeogeogr. Palaeoclimatol. Palaeoecol. 259, 93-95.

Desprat, S., Sánches-Goñi, M.F., Loutre, M.F., 2003. Revealing climatic variability in the last three millennia in northwestern Iberia using pollen influx data. Earth Planet. Sci. Lett. 213, 63-78.

Dhal, S.O., Bakke, J., Lie, O., Nesje, A., 2003. Reconstruction of former glacier equilibrium-line altitudes based on proglacial sites: an evaluation of approaches and selection of sites. Quat. Sci. Rev. 22, 275-287.

Ego, F., Sebrier, M., Carey-Gailhardis, E., Beate, B., 1996. Do the Billecocha normal faults (Ecuador) reveal extension due to lithospheric body forces in the northern Andes? Tectonophysics 265, 255-373.

Evans, N.G., Gleizes, G., Leblanc, D., Bouchez, J.L., 1998. Syntectonic emplacement of the Maladeta granite (Pyrenees) deduced from relationships between Hercynian deformation and contact metamorphism. J. Geol. Soc. 155, 209-216.

Fanetti, D., Anselmetti, F.S., Chapron, E., Sturm, M., Vezzoli, L., 2008. Megaturbidite deposits in the Holocene basin fill of Lake Como (Southern Alps, Italy). Palaeogeogr. Palaeoclimatol. Palaeoecol. 259, 323-340.

Filippi, M.L., Lambert, P., Hunziker, J., Kübler, B., Bernasconi, S., 1999. Climatic and anthropogenic influence on the stable isotope record from bulk carbonates and ostracodes in Lake Neuchâtel, Switzerland, during the last two millennia. J. Paleolimnol. 21, 19-34.

Froelich, P.N., Klinkhammer, G.P., Bender, M.L., Luedtke, N.A., Heath, G.R., Cullen, D., Dauphin, P., Hammond, D., Hartman, B., Maynard, V., 1979. Early oxidation of organic matter in pelagic sediments of the eastern equatorial Atlantic: suboxic diagenesis. Geochim. Cosmochim. Acta 43, 1075-1090.

García-Ruiz, J.M., Valero-Garcés, B.L., Martí-Bono, C., González-Sampériz, P., 2003. Asynchroneity of maximum glacier advances in the central Spanish Pyrenees. J. Quat. Sci. 18, 61-72.

Gil-García, M.J., Ruiz-Zapata, M.B., Santisteba, J.I., Mediavilla, R., López-Pamo, E., Dabrio, C.J., 2007. Late Holocene environments in Las Tablas de Daimiel (south central Iberian peninsula, Spain). Veget. Hist. Archaeobot. 16, 241-250.

González-Sampériz, P., Valero-Garcés, B., Moreno, A., Jalut, G., García-Ruiz, J.M., Martí-Bono, C., Delgado-Huertas, A., Navas, A., 2006. Climate variability in the Spanish Pyrenees during the last 30,000 yr revealed by the El Portalet sequence. Quat. Res. 66, 38-52.

Gutiérrez-Elorza, M., Peña-Monné, J.L., 1998. Geomorphology and Late Holocene climatic change in Northeastern Spain. Geomorphology 23, 205-217.

IGN, 2006. Servicio de información s´ismica del Instituto Geográfico Nacional de España (http://www.ign.es/ign/es/IGN/SisIndice.jsp).

Lanci, L., Hirt, A.M., Lowrie, W., Lotter, A.F., Lemcke, G., Sturm, M., 1999. Mineral-magnetic record of Late Quaternary climatic changes in a high Alpine lake. Earth Planet. Sci. Lett. 170, 49-59.

Larrasoaña, J.C., Roberts, A.P., Stoner, J.S., Richter, C., Wehausen, R., 2003. A new proxy for bottom-water ventilation in the eastern Mediterranean based on diagenetically controlled magnetic properties of sapropel-bearing sediments. Palaeogeogr. Palaeoclimatol. Palaeoecol. 190, 221-242.

Larrasoaña, J.C., Roberts, A.P., Musgrave, R.J., Gràcia, E., Piñero, E., Vega, M., Martínez-Ruiz, F., 2007. Diagenetic formation of greigite and pyrrhotite in gas hydrate marine sedimentary systems: results from ODP Leg 204 (southern Hydrate Ridge). Earth Planet. Sci. Lett. 261, 350-366.

Leblanc, D., Gleizes, G., Lespinasse, P., Olivier, P., Bouchez, J.L., 1994. The maladeta granit polydiapir, Spanish Pyrenees: a detailed magneto-structural study. J. Struct. Geol. 16, 223-235.

Leemann, S., Niessen, F., 1994. Holocene glacial activity and climatic variations in the Swiss Alps: reconstructing a continuous record from proglacial lake sediments. The Holocene 4, 259-268.

Leonard, E.M., Reasoner, M.A., 1999. A continuous Holocene glacial record inferred from proglacial lake sediments in Banff National park, Alberta, Canada. Quat. Res. 51, 1-13.

Lie, O., Dhal, S.O., Nesje, A., Matthews, J.A., Sandvold, S., 2004. Holocene fluctuations of a polythermal glacier in high-alpine eastern Jotunheim, central-southern Norway. Quat. Sci. Rev. 23, 1925-1945.

Matthews, J.A., Karlén, W., 1992. Asynchronous Neoglaciation and Holocene climate change reconstructed from Norwegian glacio-lacustrine sedimentary sequences. Geology 20, 991-994.

Mollard, J.D., 1977. Regional landslide types in Canada. Rev. Engin. Geol. 3, 29-56.

Monecke, K., Anselmetti, F., Becker, A., Sturm, M., Giardini, D., 2004. Signature of historic earthquakes in lake sediments in central Switzerland. Tectonophysics 394, 21-40.

Morellón, M., Valero-Garcés, B., Moreno, A., González-Sampériz, P., Mata, P., Romero, O., Maestro, M., Navas, A., 2008. Holocene palaeohydrology and climate variability in northeastern Spain: the sedimentary record of Lake Estanya (Pre-Pyrenean range). Quat. Int. 181, 15-31.

Moya, J., Vilaplana, J.M., 1992. Tectónica reciente en el macizo de la Maladeta, sector del Alto Esera (Pirineo Central). In: Cearreta, A., Ugarte, F.M. (Eds.), The Late Quaternary in the Western Pyrenean Region. Servicio Editorial Universidad del País Vasco, Bilbao, Spain, pp. 385-403.

Nesje, A., Bjune, A.E., Bakke, J., Dhal, S.O., Lie, O., Birks, H.J.B., 2006. Holocene palaeoclimate reconstructions at Vanndalsvatnet, western Norway, with particular reference to the 8200 cal. yr BP event. The Holocene 16, 717-729.

Ortuño, M., Queralt, P., Martí, A., Ledo, J., Masana, E., Perea, H., Santanach, P., 2008. The North Maladeta Fault (Spanish Central Pyrenees) as the Vielha 1923 earthquake seismic source: recent activity revealed by geomorphological and geophysical research. Tectonophysics 45, 246-262.

Pallàs, R., Rodés, A., Braucher, R., Carcaillet, J., Ortuño, M., Bordonau, J., Bourlès, D., Vilaplana, J.M., Masana, E., Santanach, P., 2006. Late Pleistocene and Holocene glaciation in the Pyrenees: a critical review and new evidence from ^{10}Be exposure ages, south-central Pyrenees. Quat. Sci. Rev. 25, 2937-2963.

Paasche, Ø, Dahl, S.O., Løvlie, R., Bakke, J., Nesje, A., 2007. Rockglacier activity during the Last Glacial-Interglacial transition and Holocene spring snowmelting. Quat. Sci. Rev. 26, 793-807.

Paterson, W.S.B., 1994. The Physics of Glaciers. Pergamon Press, Oxford.

Persaud, M., Pfiffner, O.A., 2004. Active deformation in the eastern Swiss Alps: post-glacial faults, seismicity and surface uplift. Tectonophysics 385, 59-84.

Peters, C., Dekkers, M.J., 2003. Selected room temperature magnetic parameters as a function of mineralogy, concentration and grain size. Phys. Chem. Earth 28, 659-667.

Pla, S., Catalan, J., 2005. Chrysophyte cysts from lake sediments reveal the submillenial winter/spring climate variability in the northwestern Meditterranean region throughout the Holocene. Clim.Dyn. 24, 263-278.

Riera, S., Wansard, G., Julià, R., 2004. 2000-year environmental history of a karstic lake in the Mediterranean pre-Pyrenees: the Estanya lakes (Spain). Catena 55, 293-324.

Roberts, A.P., 1995. Magnetic properties of sedimentary greigite (Fe_3S_4). Earth Planet. Sci. Lett. 144, 7-17.

Roberts, A.P., Weaver, R., 2005. Multiple mechanisms of remagnetization involving sedimentary greigite (Fe_3S_4). Earth Planet. Sci. Lett. 231, 263-277.

Snowball, I.F., 1991. Magnetic hysteresis properties of greigite (Fe_3S_4) and a new occurrence in Holocene sediments from Swedish Lappland. Phys. Earth Planet. Inter. 68, 32-40.

Snowball, I.F., 1993. Mineral magnetic properties of Holocene lake sediments and soils from the Kårsa valley, Lapland, Sweden, and their relevance to palaeoenvironmental reconstruction. Terra Nova 5, 258-270.

Snowball, I.F., 1994. Bacterial magnetite and the magnetic properties of sediments in a Swedish lake. Earth Planet. Sci. Lett. 126, 129-142.

Snowball, I., Sandgren, P., Petterson, G., 1999. The mineral magnetic properties of an annually laminated Holocene lake-sediment sequence in northern Sweeden. The Holocene 9, 353-362.

Souriau, A., Pauchet, H., 1998. A new synthesis of Pyrenean seismicity and its tectonic implications. Tectonophysics 290, 221-244.

Stuiver, M., Reimer, P.J., 1986. A computer program for radiocarbon age calibration. Radiocarbon 28, 1022-1030.

Stuiver, M., Reimer, P.J., Reimer, R.W., 2005. CALIB Radiocarbon Calibration version 5.0. University of Washington Quaternary Isotope Lab (www.calib.org/).

Thompson, R., Oldfield, F., 1986. Environmental Magnetism. Allen and Unwin, London.

Ustaszewski, M., Hampel, A., Pfiffner, O.A., 2008. Composite faults in the Swiss Alps formed by the interplay of tectonics, gravitation and postglacial rebound: an integrated field and modelling study. Swiss. J. Geosci. in press.

Verosub, K.L., Roberts, A.P., 1995. Environmental magnetism: past, present and future. J. Geophys. Res., 100, 2175-2192.

Villar, L., Sesé, J.A., Ferrández, J.V., 1997. Atlas de la flora del Pirineo aragonés, I: consejos de protección de la naturaleza de Aragón. Inst. Est. Altoaragoneses, Huesca.

Wagner, B., Reicherter, K., Daut, G., Wessels, M., Matzinger, A., Schwalb, A., Spirkovski, S., Sanxhaku, M., 2008. The potential of Lake Ohrid for long-term palaeoenvironmental reconstructions. Palaeogeogr. Palaeoclimatol. Palaeoecol. 259, 341-356.

Wells, D.L., Coppersmith, K.J., 1994. New empirical relationships among magnitude, rupture length, rupture area and surface displacement. Bull. Seismol. Soc. Am. 84, 974-1002.

Wright, H.E., 1980. Cores of soft lake sediments. Boreas 9, 107-114.

Zhu, L.P., Zhang, P.Z., Xia, W.L., Li, B.Y., Chen, L., 2003. 1400-year cold/warm frluctuations reflected by environmental magnetism of a lake sediment core from the Chen Co, southern Tibet, China. J. Paleolimnol. 29, 391-401.

Figure Captions

Figure 1. A) Sketch map showing historical large earthquakes (I > VIII) in the Pyrenean region (IGN, 2006). The studied area, indicated by a black square, includes two of the greater earthquakes occurred in the Pyrenees. B) Ortophoto of the studied area, with indication of the boundary between the Maladeta granitoid and the paleozoic country rocks and location of two historical earthquakes (small triangle: I = V, 2.12.1919; large triangle: Ribagorza earthquake, I = VIII-IX, 3.3.1373). C) Geology and geomorphology of the Maladeta Massif (after Moya and Vilaplana, 1992; Copons and Bordonau, 1994, 1996; Chueca et al., 2005), with location of Lake Barrancs and core B5. The dashed line indicates the lake catchment. C) Aerial picture showing the main structural and geomorphological features around Lake Barrancs.

Figure 2. A) Lake Barrancs and its deltaic plain (DP) as viewed from the south, with location of core B5. B) Lake Barrancs viewed from the north. The Tempestats glacier (TG), the Little Ice Age (LIA) and the Holocene (H) moraines are clearly visible. C) Detail of two of the recent faults (f) located near the SW shore of Lake Barrancs. D) Detail of the drilling camp and platform set up over the frozen surface of the lake.

Figure 3. Lithostratigraphy, sedimentary facies, radiocarbon dates, and selected magnetic properties of core B5.

Figure 4. Age-depth model for core B5. Shading in the left column indicates different sedimentary facies (see Figure 3).

Figure 5. Age variations of selected magnetic properties from core B5, which have been compared with a regional climatic record of winter mean temperatures (Lake Redon, Pla and Catalan, 2005) and the sequence of climate periods recorded in the Iberian Peninsula (Gutiérrez-Elorza and Peña-Monné, 1998; Riera et al., 2002; Desprat et al., 2003; Gil-García et al., 2007). The left column indicates the timing of historical earthquakes recorded in the area and the timing of the two additional earthquakes inferred from the occurrence of facies F3 paleosoils. The box marked by LIA indicates the extent of the Little Ice Age in the Maladeta Massif (after Copons and Bordonau, 1994, 1996; Chueca et al., 2005).

Figure 6. Sketches summarizing the recent tectonic and geomorphologic evolution of the Lake Barrancs basin, both in map view and in cross section (A-A′), as inferred from results from core B5 and from previous studies by Moya and Vilaplana, 1992; Copons and Bordonau, 1994, 1996; Chueca et al., 2005). P_1 and P_2 in the sketches representing the Late Holocene (A.D.

300) and the maximum glacier advance during the Little Ice Age (A.D. 1820; Chueca et al., 2005) denote faults projected into the cross section A-A´.

Tables

Table 1. TOC content of samples representative for the three facies types recovered in core B5.

Table 2. Macrofossil plants and invertebrate remains in two selected samples from the organic-rich layer between 344 and 363 cblf.

Table 3. Radiocarbon data from core B5.

Figure 1

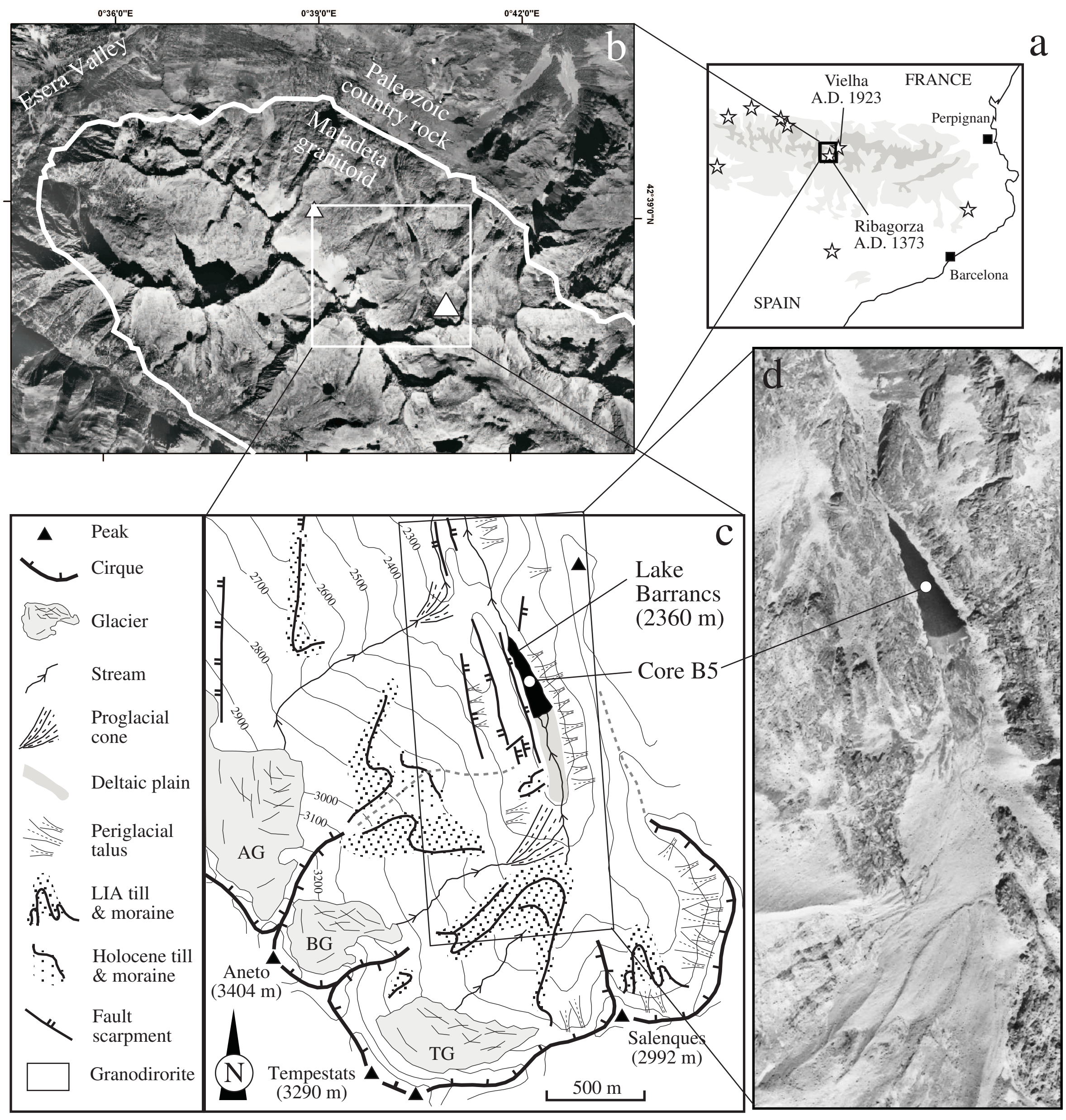

Figure 1
Larrasoa a et al.

Figure 2

Figure 2
Larrasoa a et al.

Figure 3

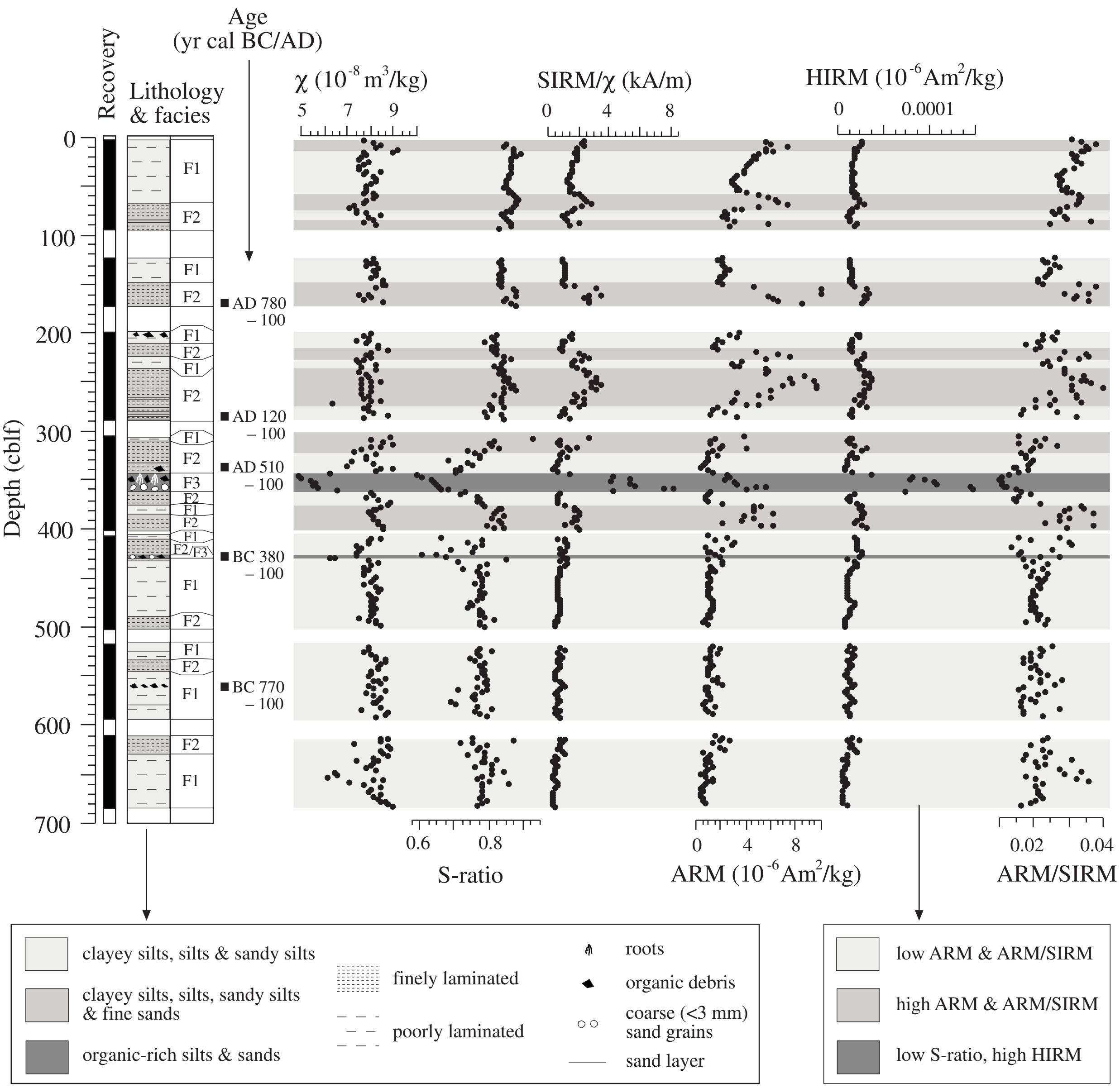

Figure 3
Larrasoa a et al.

Figure 4

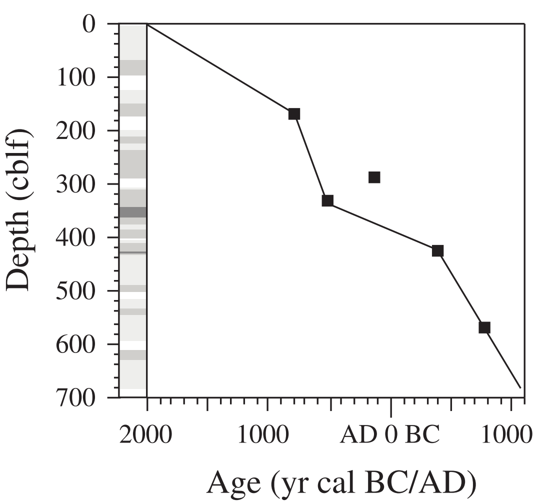

Figure 4
Larrasoa a et al.

Figure 5

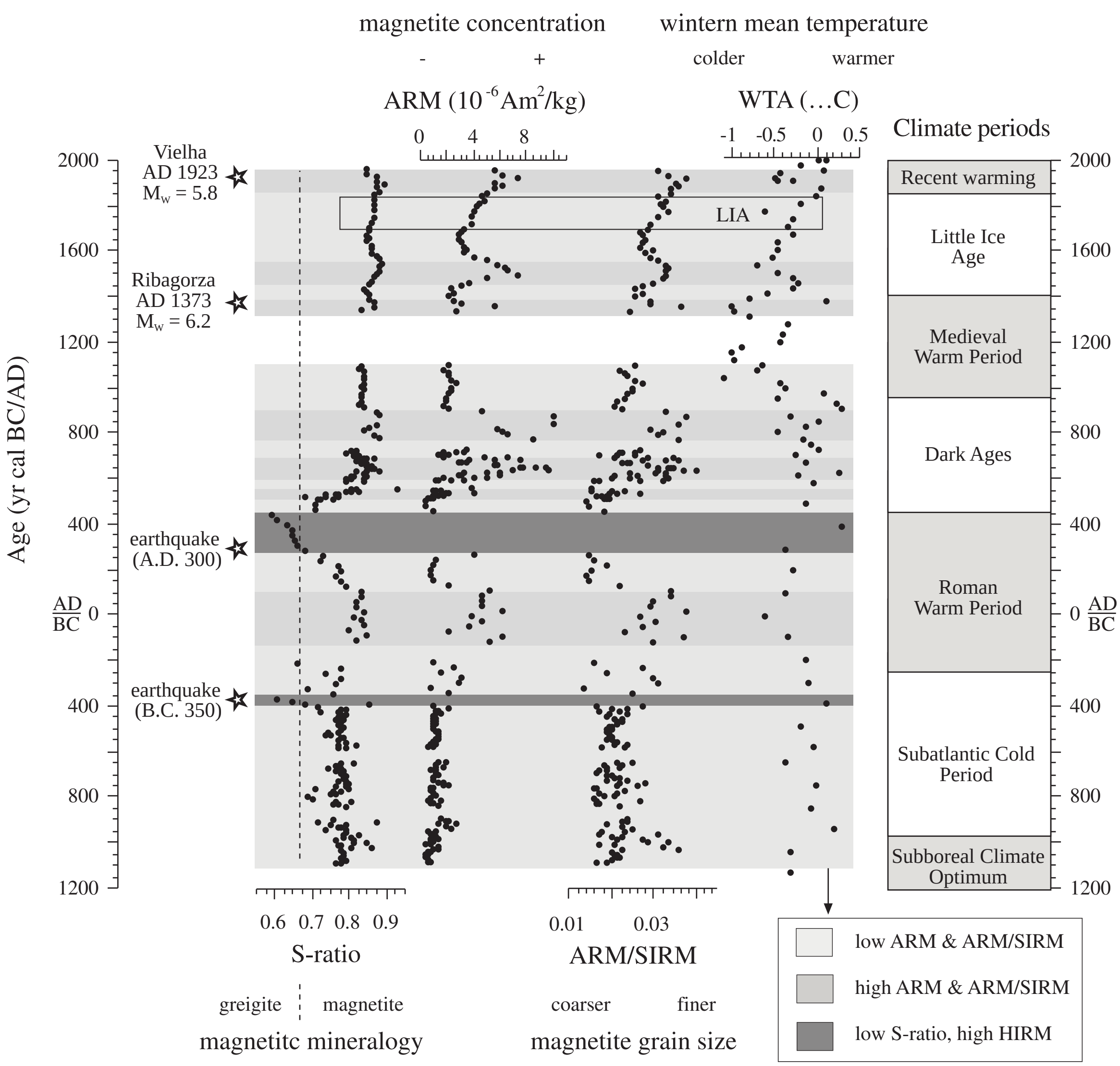

Figure 5
Larrasoa a et al.

Figure 6

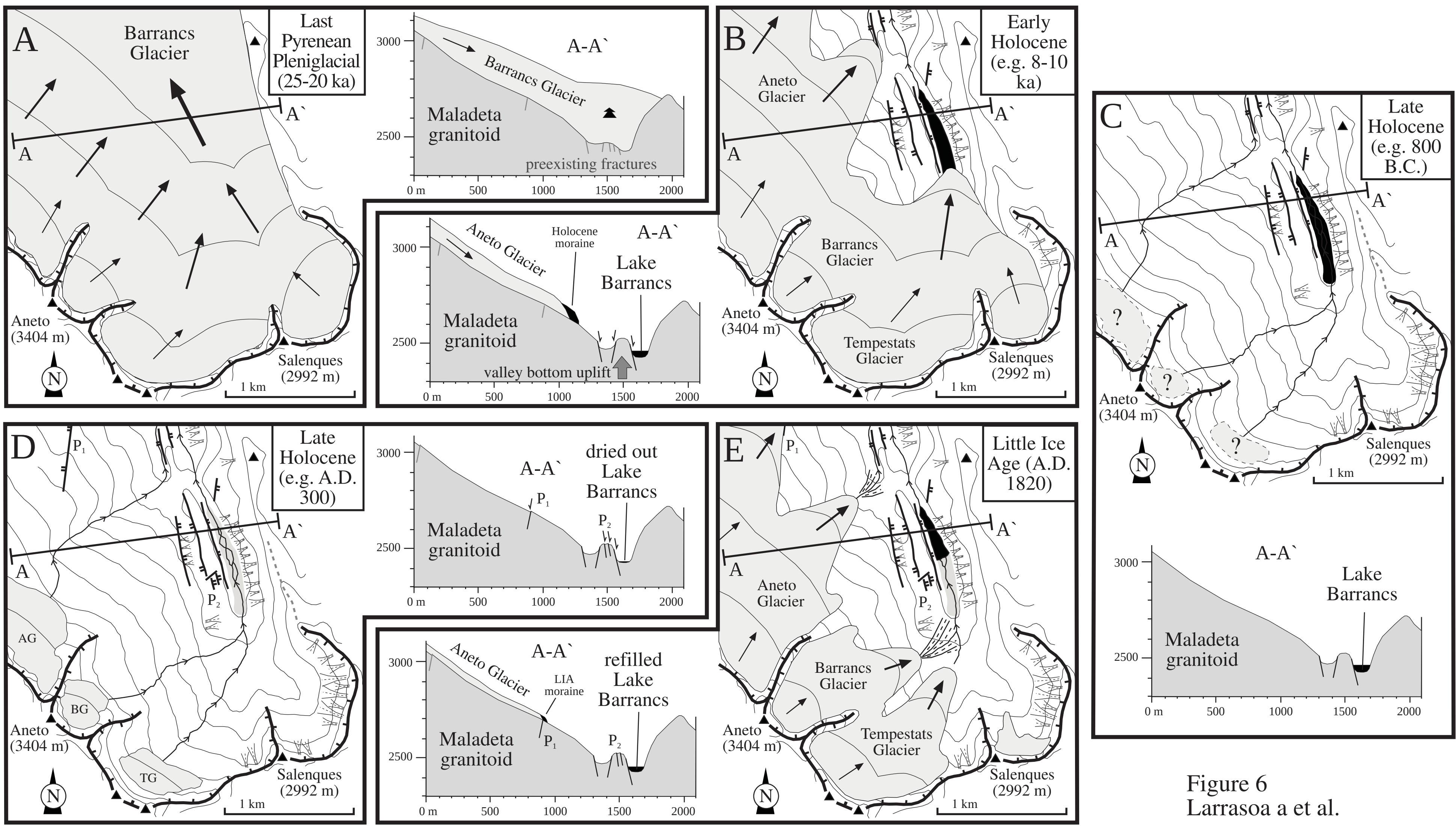

Figure 6
Larrasoa a et al.

Table 1

Table 1. TOC content of samples representative for the three facies types recovered in core B5.

Sample	Depth (cblf)	Facies type	TOC (%)
3.25	254	F2	0.36
4.20	349	F3	2.59
4.22	353	F3	2.7
7.18	650	F1	0.3

Table 2
Click here to download Table: Table 2.xls

Table 2. Macrofossil plants and invertebrate remains in two selected samples from the organic-rich layer between 344 and 363 c

		Macrofossil plants			Other constituents	
Sample	Depth (cm)	Plant type	Plant part	Abundance	Invertebrate remains	Abundance
4.18	345	*Calluna vulgaris*	seeds	1	Oribatid mites	f
		Calluna vulgaris	flowers	3	Chironomids	vr
		Calluna vulgaris	leaves, stems, twig	f	Insect fragments	p
		Juniperus communis	leaves	4		
		Salix sp.	bark fragments	r		
		Betula (peduncula/pubescens)	bud scales	3		
		Rhododendron ferrugineum	leaf glands	oc		
		Rhododendron ferrugineum	seeds	2		
		Rhododendron cf. ferrugineum	leaf fragments	oc		
		Ranunculus sp.	achene (small)	1		
		Carex sp. (tristigmata)	nutlets	1		
		Roots		oc		
		Leaf and twig fragments		1		
4.26	362	*Calluna vulgaris*	twigs	oc	Chironomids	r
		Selaginella selaginoides	megaspores	2	Trichoptera	vr
		Twigs		oc	Insect fragments	p
		Leaf fragments		oc		

f = frequent
oc = occasional
r = rare
vr = very rare
p = present

Table 3
Click here to download Table: Table 3.xls

Table 3. Radiocarbon data from core B5.

Lab. Ref.	Depth (cblf)	Material	14C age (year B.P.)	cal. Age (2σ)	Prob. Distrib.	$\delta^{13}C$ (‰)
BETA-122150	170	Bulk sediment	1240 ± 40	**AD 680-882**	**1**	-26.3
BETA-122151	286.5	Bulk sediment	1900 ± 50	**AD 3-235 ***	**1**	-26.7
BETA-122153	338	Plant material	1540 ± 30	**AD 430-590**	**1**	-27.2
BETA-122148	426	Bulk sediment	2300 ± 40	**BC 412-347**	**0.622**	-26.5
				BC 318-207	0.378	
BETA-122149	567	Plant material	2560 ± 40	**BC 809-729**	**0.501**	-26.4
				BC 692-659	0.157	
				BC 652-543	0.342	

Bold numbers indicate radiocarbon ages chosen on the basis of their probability distribution.

The asterisk denotes an inverted age.